Proceedings of the Symposium A of the European Materials Research, Warsaw, September 2008

Damage Assessment in Low Doses $^{30}Si^{+}$-Implanted GaAs

D. Desnica Frankovića,*, V. Desnicab and K. Furića

[a]Materials Physics Department, R. Boškovic Institute

Bijenička 54, P.O. Box 180, 10000 Zagreb, Croatia

[b]Department for Conservation and Restoration, Academy of Fine Arts

Ilica 85, 10000 Zagreb, Croatia

Ion implantation is a widely used technique in device technology, and becoming even more important as the size of devices decreases. The studies of damage and introduced defects have been extensive and, although the overall development and annealing of the implantation damage is relatively well understood, many details remain unclear. Especially, not enough attention has been paid to the effects of very low doses, which are particularly important in controlling the threshold voltage of transistors in the fabrication of GaAs integrated circuits. The reason might be that the induced changes were very often below the detectivity limits of standard methods. In this work, we present the disorder analysis, conducted on GaAs implanted with low ion doses. Czochralski grown, undoped, (100) oriented GaAs samples were implanted with 100 keV $^{30}Si^{+}$ ions, doses ranging from $3 \times 10^{11}/cm^2$–$3 \times 10^{13}/cm^2$, at 21°C. The damage assessment was done by applying Raman scattering and Rutherford backscattering ion channeling (RBS), linked by the inter-cascade distance model and the results were then compared with the results of photoacoustic displacement technique. We have shown that Raman scattering is very sensitive method even if applied on samples implanted with very low doses. Furthermore, the equivalency between the Raman scattering and Rutherford backscattering damage assessment, previously established for high doses *via* the inter-cascade distance model, proved equally valid also for very low implantation doses, where implanted ions create disordered cascades that are far apart, and most of the layer is still undamaged.

PACS numbers: 78.30.Ly, 61.72.Vv, 63.50.+x

1. Introduction

Present-day microelectronic devices are predominantly based on doped semiconductors that are of tremendous technological importance. In that sense, ion implantation is a widely used technique in device technology. In particular, ion implantation of Si is extensively employed in the fabrication of high-speed GaAs integrated circuits, so, the thorough understanding of doping mechanism could allow tuning of the electronic properties according to the technological needs [1, 2]. Furthermore, formation of patterned doping layers buried in semiconductors is important for fabrication of three-dimensional nano-electronic devices such as coupled electron waveguides. By using focused ion beam (FIB) implantation, impurities can be doped masklessly at selected areas on semiconductor surfaces, and the doped layers can be buried by successive overlayer regrowth [3, 4]. In this process, reduction of damages introduced by the FIB irradiation, should be necessary to obtain higher doping efficiency.

Being a very violent procedure, implantation introduces a variety of defects, disorder and damage into the material. Defects introduced during implantation have a central role in many aspects of ion implantation processing, notably in annealing and transient-enhanced diffusion behavior, which could limit the ability to fabricate shallow junctions for ultra-large-scale-integrated circuits. The studies of damage and introduced defects have been extensive and, although the overall development and annealing of the implantation damage is relatively well understood, many details remain unclear. Especially, not enough attention has been paid to the effects of very low doses, which are particularly important in controlling the threshold voltage of transistors in the fabrication of GaAs integrated circuits. The reason might be that the induced changes were very often below the detectivity limits of standard methods. Application of some specific techniques, like photoacoustic displacement (PAD) [5], has shed more light on this issue. In parallel, Raman spectroscopy (RS) has been established as a very efficient and a very sensitive method for the detection of damage in crystal structure and has been used successfully in this type of investigations [6]. In this work we present the results of the implantation induced disorder analysis, conducted on low dose Si^{+}-implanted GaAs, by applying Raman scattering and Rutherford backscattering ion channeling (RBS), connected by the inter-cascade distance model (ICD) and compared with the results of PAD.

* corresponding author; e-mail: ddesnica@irb.hr

2. Experimental

A series of monocrystalline liquid encapsulated Czochralski grown, undoped, (100) oriented GaAs samples, with dislocation density in the $10^4/\mathrm{cm}^2$ range, was implanted with 100 keV $^{30}Si^{+}$ ions, doses ranging from $3\times10^{11}/\mathrm{cm}^2$–$3\times10^{13}/\mathrm{cm}^2$, at 21°C (room temperature, RT). The substrates were tilted 7° with respect to the incident beam to minimize channeling effects. After the implantation, the samples were initially characterized by RBS and then analyzed by RS.

Raman spectra were excited using argon-ion laser Coherent Inc. model Innova 100; its line of 514.5 nm wavelength (2.41 eV) was filtered by Anaspec's double-pass premonochromator to reduce spurious plasma lines. The beam was focused using astigmatic lens, in near grazing 90° scattering geometry, to elliptic (not circular) spot size of approximately 50×3000 $\mu\mathrm{m}^2$ similarly to the concept of line focusing. Incident polarization was perpendicular to the scattering plane. In this way it was possible to keep the beam power of 0.14 W at the sample place with no danger of overheating. All spectra were recorded with computerized triple monochromator DILOR model Z24 improved by Peltier-cooled C31034 RCA photomultiplier, specially selected for single photon counting. Most of spectra were recorded in 3 scans, with accumulation time of 3 s, with step size of 1 cm^{-1} and using slit width of 3 cm^{-1}.

The spectra were taken in the 190 to 320 cm^{-1} range. This, or similarly limited frequency range, is often used in Raman analysis [7–10] since in this range the characteristic signals from all crystalline and amorphous fractions of implanted GaAs layer can be observed, including two crystalline modes (longitudinal optical LO(Γ) peak at 290 cm^{-1}, and transversal optical TO(Γ) at 268 cm^{-1}), and the most prominent amorphous band (centered at 250 cm^{-1}).

For ion channeling (RBS), backscattered ions from a 2 MeV He^{+} beam were detected at a scattering angle of 160°. The probing beam was aligned with the ⟨100⟩ axis of the crystal. Damage profiles were extracted from the RBS spectra by subtracting the dechanneling portion of the yield, and correcting for the dechanneled fraction of the beam as a function of depth.

3. Results and discussion

In Fig. 1, a gamut of first-order Raman spectra is presented; depicting ion dose effects on representative samples. Following implantation, the crystalline LO(Γ) line, located at 290 cm^{-1} in undamaged sample, shifts to the lower frequency, attenuates and broadens. With increasing the fluency, other features emerge in the spectra, particularly the TO peak at 268 cm^{-1}, which is symmetry-forbidden in the (100)-oriented monocrystalline zinc blende structure. In that case the phonons which are not located at the Γ point of the Brillouin zone significantly contribute to the Raman spectrum as well. Therefore,

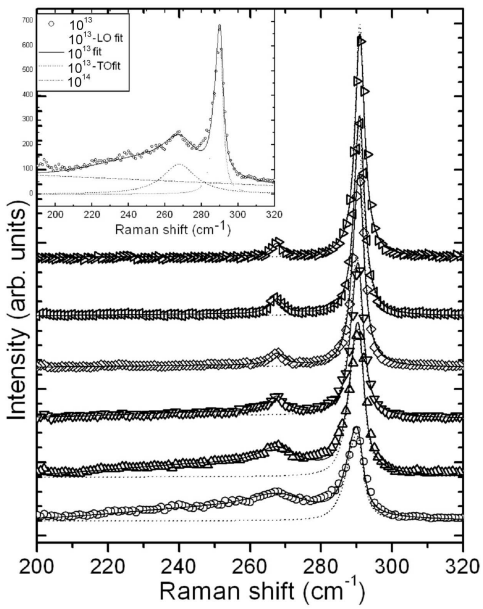

Fig. 1. Raman spectra of the 100 keV $^{30}Si^{+}$-implanted GaAs, obtained using 2.41 eV excitation line. The implantation doses are denoted with the following symbols: ○ 10^{13}; Δ 9×10^{12}; ▽ 3×10^{12}; ◇ 10^{12}; ◀ 3×10^{11}; ▶ unimplanted. Lines represent corresponding fits. Inset: an example of the deconvolution procedure, explained in the text.

in this analysis, denotation LO(Γ) and TO(Γ) was not further used.

The TO peak shows very small red shift and only slight broadening, in accord with previous reports [10]. We have interpreted it as a scattering from those parts of the implanted layer which were re-crystallized, and misoriented after freezing out of the hot tracks along the ions' path. A broad band at 250 cm^{-1}, which is characteristic for the continuous-random-network structure of the amorphous phase (a-CRN) [7], is present only in the 1×10^{13} and 3×10^{13} ions $/\mathrm{cm}^2$ implanted samples. Thus, only at those doses the amorphous fraction contributes, albeit slightly, to the RS signal.

In order to analyze disorder quantitatively the RS spectrum was deconvoluted into the following contributions: background signal approximated with a linear function, the a-CRN signal with a Gaussian function, and the TO crystalline peak with a Lorentzian shape function, whereas the LO phonon peak was simulated by the phonon confinement model. An example of the deconvolution procedure is shown as an inset in Fig. 1.

For a quantitative disorder assessment, the average size of the undamaged crystalline regions, L_{RS}, over which order and translational symmetry is preserved, could be determined from the analysis of the LO phonon peak. The LO peak was analyzed within the "spatial correlation" model [11–13] in which it is assumed that defects introduced by irradiation partition the crystal into regions of a finite size L. Due to the loss of a long range

order, the symmetry conservation rule spans only a certain range of wave numbers of the order of $1/L$, where L is the correlation (localization) length, i.e. an average size of the undamaged region. This leads to a relaxation of the symmetry-related selection rules and the momentum conservation so that all phonons in the Brillouin zone participate in the first order scattering. In other words, the $\boldsymbol{q} \neq 0$ phonons — in GaAs determined by the dispersion relation $\omega(\boldsymbol{q}) = A + B\cos(\pi q)$ [11] ($A = 267.8$ cm^{-1} and $B = 22.5$ cm^{-1}) [6] — also become Raman-active. The localization of the wave vector is imposed through the Gaussian attenuation function $\exp(-q^2L^2/4a^2)$ and the Raman intensity at frequency ω is expressed as

$$I(\omega) \propto \int_0^1 \exp\left(\frac{-q^2L^2}{4a^2}\right) \frac{\mathrm{d}^3 q}{[\omega - \omega(q)]^2 + (\Gamma_0/2)^2}, \quad (1)$$

where $\boldsymbol{q}$ is the wave vector in the units of $2\pi/a$, a is the lattice constant ($a = 5.65$ Å for GaAs crystal), Γ_0 is the FWHM of the unperturbed LO shape and determined from the measurement on undamaged crystal ($\Gamma_0 \approx 3.2$ cm^{-1}). Using the above equations, we have calculated FWHM versus the mean size of undamaged regions L, depicted in Fig. 2 as a solid line. For our experimental results, the integration is performed numerically and for each dose, the correlation length is obtained as a parameter of the fitting curve calculated after Eq. (1). The results for low doses are denoted by a symbol ▽. In the same figure, the results from Ref. [6], obtained by the identical procedure but for high-dose implantations are presented, denoted by ○.

The dependence of the LO peak position, PP, versus the average size of the undamaged region L, is presented as an inset in Fig. 2. Besides the changes in the phonon localization length L, ion implantation could induce the defect-associated lattice strains [10].

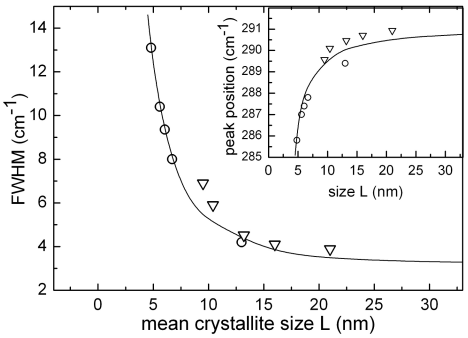

Fig. 2. Dependence of the FWHM on the correlation length L. Solid line is obtained from Eq. (1). The results for low doses are denoted by ▽. The results from Ref. [6], obtained for high-dose implantations are denoted by ○. Inset: the dependence of the LO-peak position, PP, versus the average size of the undamaged region L. ▽ — experimental values; ○ values for high implantation doses from Ref. [6]; solid line — from the theoretical formula.

The PP is very sensitive to the internal stress in the matrix, which causes an upward shift of the crystalline peak, thus potentially compensating the downward shift of phonon frequency caused by confinement. Since the theoretical curve predicts the experimental results fairly well, it could be concluded that the changes in peak frequency are predominantly affected by the phonon confinement effects and that the strain effects have minimal influence on the LO peak position.

Quantitative disorder assessment from the analysis of undamaged crystalline regions in Raman scattering could be compared with an analogous parameter, L_{RBS}, calculated from the RBS. The RBS detects atoms that are displaced from their crystal-lattice sites. Disorder then can be expressed as the fraction of atoms that are displaced, with unity corresponding to completely amorphized layer. RBS is thus a non-specific technique that detects all types of crystalline disorder, although with some variation in sensitivity, giving a quantitative estimate of the total disorder. Unfortunately, RBS, which is a standard method for damage assessment, is insensitive at very low doses, the detection limit being typically 5×10^{13} ions/cm^2, so the simple comparison with L_{RS} in the low-dose range is not possible.

However, if we apply an, independently introduced, ICD model which estimates the average distance, L_{ICD}, between the implantation-induced cascades as a function of ion dose, this analysis could be performed [6]. The ICD model follows the classical approach of Morehead and Crowder [14] where ion irradiation produces a cylinder-like disorder region around an ion trajectory, of the volume: $A_{\mathrm{a1}}d$, where A_{a1} is the average amorphized single cascade area (projected on the surface of the crystal), and d is the thickness of the implanted layer. The amorphized part of the total area, A_{tot} depends on the applied dose, D, as $A_{\mathrm{a}} = A_{\mathrm{a1}}DA_{\mathrm{tot}}$, leading to an estimate of the critical amorphization dose $D_{\mathrm{c}} = 1/A_{\mathrm{a1}}$, for which the whole implanted area should be amorphous. When an allowance is made for the cascades which overlap with preexisting amorphous areas [15], the effective cumulative amorphized area, $A_{\mathrm{a,eff}}$, covered by cascades is

$$A_{\mathrm{a,eff}} = A_{\mathrm{tot}}[1 - \exp(-A_{\mathrm{a1}}D)]. \quad (2)$$

Since the partition of the implanted layer thus reduces to two-dimensional problem, the average distance between the disordered cascades L can be estimated from $L = 1/D^{1/2}$. For higher doses, when the probability for the overlap of different cascades becomes significant, the new cascades become less efficient in partitioning the remaining undamaged parts and an effective dose, D_{eff}, can be defined as $D_{\mathrm{eff}} = D_{\mathrm{c}}[1 - \exp(-D/D_{\mathrm{c}})]$. Then the effective inter-cascade distance, L_{ICD}, can be estimated from

$$L_{\mathrm{ICD}} = 1/\sqrt{Dc[1 - \exp(-D/D_{\mathrm{c}})]}. \quad (3)$$

The full line in Fig. 3 is obtained if an average single cascade diameter of 1 nm is assumed, leading to a critical dose $D_{\mathrm{c}} = 1.25 \times 10^{14}$/cm^2. Dotted line corresponds to somewhat lower value for the critical amorphization dose, D_{c}.

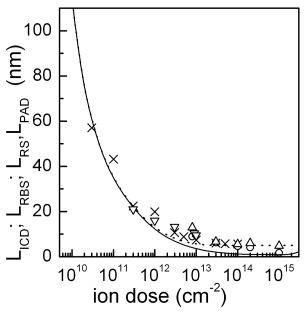

Fig. 3. Dependence of the average size of the undamaged region L on the ion dose. $\triangledown$ — L_{RS}, values of the correlation length determined from RS spectra for low doses and $\triangle$ — high doses (Ref. [6]); $\circ$ — L_{RBS}, values determined from the RBS volume disordered fraction; $\times$ — L_{PAD}, calculated from data in Ref. [5] and inter-cascade distance L_{ICD}, full line — calculated from Eq. (3) for $D_{\mathrm{c}} = 1.25 \times 10^{14}$ cm^{-2} and dotted curve with $D_{\mathrm{c}} = 3 \times 10^{12}$ cm^{-2}.

The experimental values obtained from the Raman scattering analysis are designated as L_{RS}. Additionally, the average size of undamaged regions, L_{RBS}, obtained from the analysis of ion channeling data are presented. As we have demonstrated earlier [6], a quantitative comparison between RS and RBS is possible through the combination of ICD and Morehead and Crowder (MC) models. In the MC model the RBS damage fraction, f_{RBS}, corresponds to the amorphized fraction of implanted surface, $f_{\mathrm{RBS}} = A_{\mathrm{a,eff}}/A_{\mathrm{tot}} = A_{\mathrm{tot}}[1-\exp(-A_{\mathrm{a1}}D)]/A_{\mathrm{tot}}$. Hence, from Eqs. (2) and (3) one obtains: $L_{\mathrm{RBS}} = 1/\sqrt{Dc[1-\exp(-DA_{\mathrm{a1}})]}$, or

$$L_{\mathrm{RBS}} = 1/\sqrt{(D_{\mathrm{c}} f_{\mathrm{RBS}})}. \tag{4}$$

Figure 3 depicts the average size dependence of undamaged crystal regions on ion dose. Theoretical prediction, presented by a line, is obtained from the ICD model [6], under the assumption of critical dose for amorphization $D_{\mathrm{c}} = 1.25 \times 10^{14}/\mathrm{cm}^2$. L_{RBS} values presented in Fig. 3 show reasonably good accordance with L_{ICD} — particularly with a dotted line corresponding to a lower D_{c} — and even better agreement with L_{RS}. One has to bear in mind that both L_{ICD} and L_{RS} were determined without any free, adjustable fitting parameters.

For a comparison, in Fig. 3, denoted by $\times$, we have presented results obtained by PAD technique, which measures the dose dependence of implantation-induced damage in Si implanted GaAs [5]. We have used PAD experimental points and normalized them with RBS data for one dose ($3 \times 10^{13}/\mathrm{cm}^2$) from the middle of dose range in which both methods overlap. Dose dependence of L_{PAD} (calculated by a formula analogous to equation: $L_{\mathrm{RBS}} = 1/(D_{\mathrm{c}} f_{\mathrm{RBS}})^{1/2}$) shows an excellent agreement with L_{RBS} at other doses, but also with L_{RS}, as well as with L_{ICD} particularly in low dose range. This accordance demonstrates that the correlation length concept is the same when measuring the implantation-induced disorder either by RS or RBS or PAD, and that ICD model describes well the average size of undamaged regions, L, measured by any of these three methods.

Thus, the previously established [6] equivalency between the RS and RBS damage assessment and their "connection element (relation)", the ICD model, is equally valid for very low implantation doses where implanted ions create disordered cascades that are far apart, and most of the layer is still undamaged.

4. Conclusions

The low level disorder, which was introduced in monocrystalline GaAs by implanting low doses of 100 keV Si ions, was studied by several experimental methods and theoretical models. The results of different techniques were related and mutually connected within plausible models. The influence of disorder on the Raman scattering was analyzed by fitting the LO peak with expression obtained from the spatial correlation model. For each dose, this procedure yielded the correlation length, L_{RS}, representing the mean size of crystalline regions over which the order and translational symmetry is preserved. These L_{RS} were then compared with the average undamaged distance, L_{ICD}, between the implantation-induced disorder cascades, calculated from the ICD model, which predicts damage level without free parameters. Furthermore, in dose range where the RBS measured on the same set of samples was sensitive enough that the RBS damage fraction could be estimated, the L_{RBS}, representing the average size of undamaged regions, was calculated. Finally, an analogous parameter, L_{PAD}, obtained from PAD data for low doses was determined.

Agreement between all L's, as depicted in Fig. 3, confirms that the concepts of *inter-cascade distance* and *correlation length*, each obtained from very different approaches, assumptions and approximations, are equivalent. This result then allows a meaningful and straightforward comparison of RS and RBS results but also confirms the validity of the spatial correlation model.

Acknowledgments

This research was supported by the Ministry of Science and Technology of Croatia. Authors would like to thank T.E. Haynes, Oak Ridge National Laboratory, USA for supplying implanted samples.

References

[1] X. Duan, M. Peressi, S. Baroni, *Mater. Sci. Eng. C* **26**, 756 (2006).

[2] R. Jakieła, A. Barcz, *Vacuum* **70**, 97 (2003).

[3] T. Hada, H. Miyamoto, J. Yanagisawa, F. Wakaya, Y. Yuba, K. Gamo, *Nucl. Instrum. Methods Phys. Res. B* **175-177**, 751 (2001).

[4] T. Nishiyama, Eum-Mi Kim, K. Numata, K. Pak, *Jpn. J. Appl. Phys.* **43**, L716 (2004).

[5] T. Hara, H. Muraki, S. Takeda, N. Uchitomi, Y. Kitaura, G. Gao, *Japan. J. Appl. Phys.* **33**, L1435 (1994).

[6] U.V. Desnica, I.D. Desnica, M. Ivanda, K. Furić, T.E. Haynes, *Phys. Rev. B* **55**, 16205 (1997).

[7] R. Zallen, *J. Non-Cryst. Solids* **141**, 227 (1992); R. Zallen, *The Physics of Amorphous Solids*, Wiley, New York 1983.

[8] M. Holtz, R. Zallen, O. Brafman, S. Matteson, *Phys. Rev. B* **37**, 4609 (1988).

[9] R. Ares, Y.B. Trudeau, J.L. Brebner, G.E. Kajrys, M. Jouanne, *Nucl. Instrum. Methods Phys. Res. B* **90**, 419 (1994).

[10] G. Burns, F.H. Dacol, C.R. Wie, E. Burnstein, M. Cardona, *Solid State Commun.* **62**, 449 (1987).

[11] K.K. Tiong, P.M. Amirtharaj, F.H. Pollak, D.E. Aspnes, *Appl. Phys. Lett.* **44**, 122 (1984).

[12] H. Richter, Z.P. Wang, L. Ley, *Solid State Commun.* **39**, 625 (1981).

[13] Jiqing Wang, Huibing Mao, Ziqiang Zhu, Qiang Zhao, Zhifeng Li, Wei Lu, *Appl. Surf. Sci.*, **252**, 2186 (2006).

[14] F.F. Jr. Morehead, L. Crowder, *Radiat. Eff.* **6**, 27 (1970).

[15] J.F. Gibbons, *Proc. IEEE* **60**, 1062 (1972).